Vegetation pattern formation: The mechanisms behind the forms

Ehud Meron

Citation: Physics Today **72**, 11, 30 (2019); doi: 10.1063/PT.3.4340
View online: https://doi.org/10.1063/PT.3.4340
View Table of Contents: https://physicstoday.scitation.org/toc/pto/72/11
Published by the American Institute of Physics

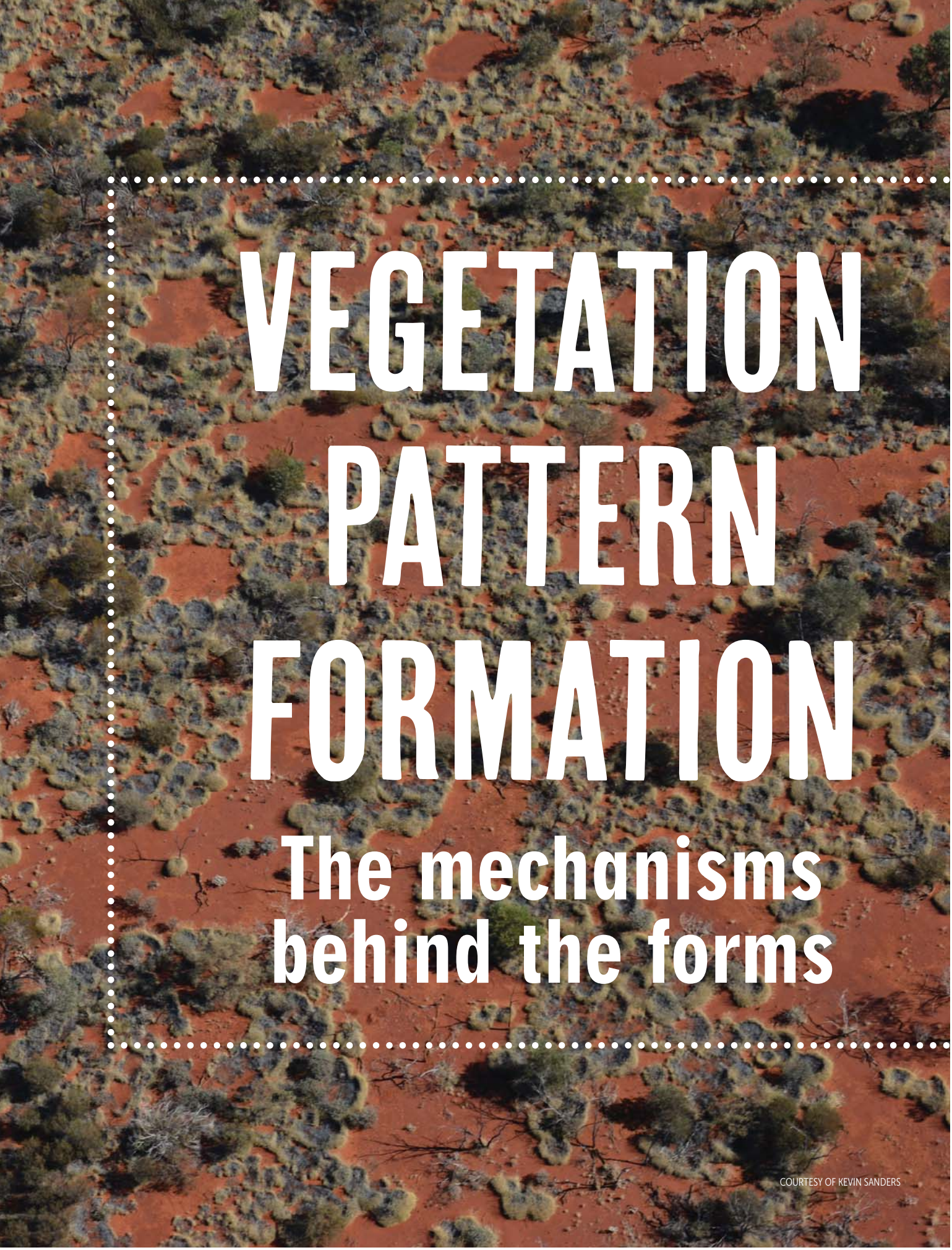

VEGETATION PATTERN FORMATION

The mechanisms behind the forms

COURTESY OF KEVIN SANDERS

Ehud Meron is a professor of physics and the Phyllis and Kurt Kilstock Chair in Environmental Physics of Arid Zones in the Jacob Blaustein Institutes for Desert Research at Ben-Gurion University of the Negev in Israel.

Ehud Meron

A simple principle relating growth to lateral water transport explains the variety of self-organized vegetation patchiness.

Mathematician Alan Turing deciphered the German Enigma code during World War II and laid the foundations of computer science as a new discipline. But toward the end of his short life, he made a lesser-known yet groundbreaking contribution. Interested in the development of patterns and shapes in biological systems, in 1952 Turing published a paper entitled "The chemical basis of morphogenesis."[1] In the theoretical study, he showed that a homogeneous system of chemical substances that react with each other and diffuse in space can self-organize into spatially periodic distributions. His work received limited attention until four decades later, when the behavior was experimentally observed.[2,3] The confirmation of Turing's prediction led to a surge in the number of studies of so-called Turing patterns, first in chemical and biological contexts and more recently in ecological contexts.[4]

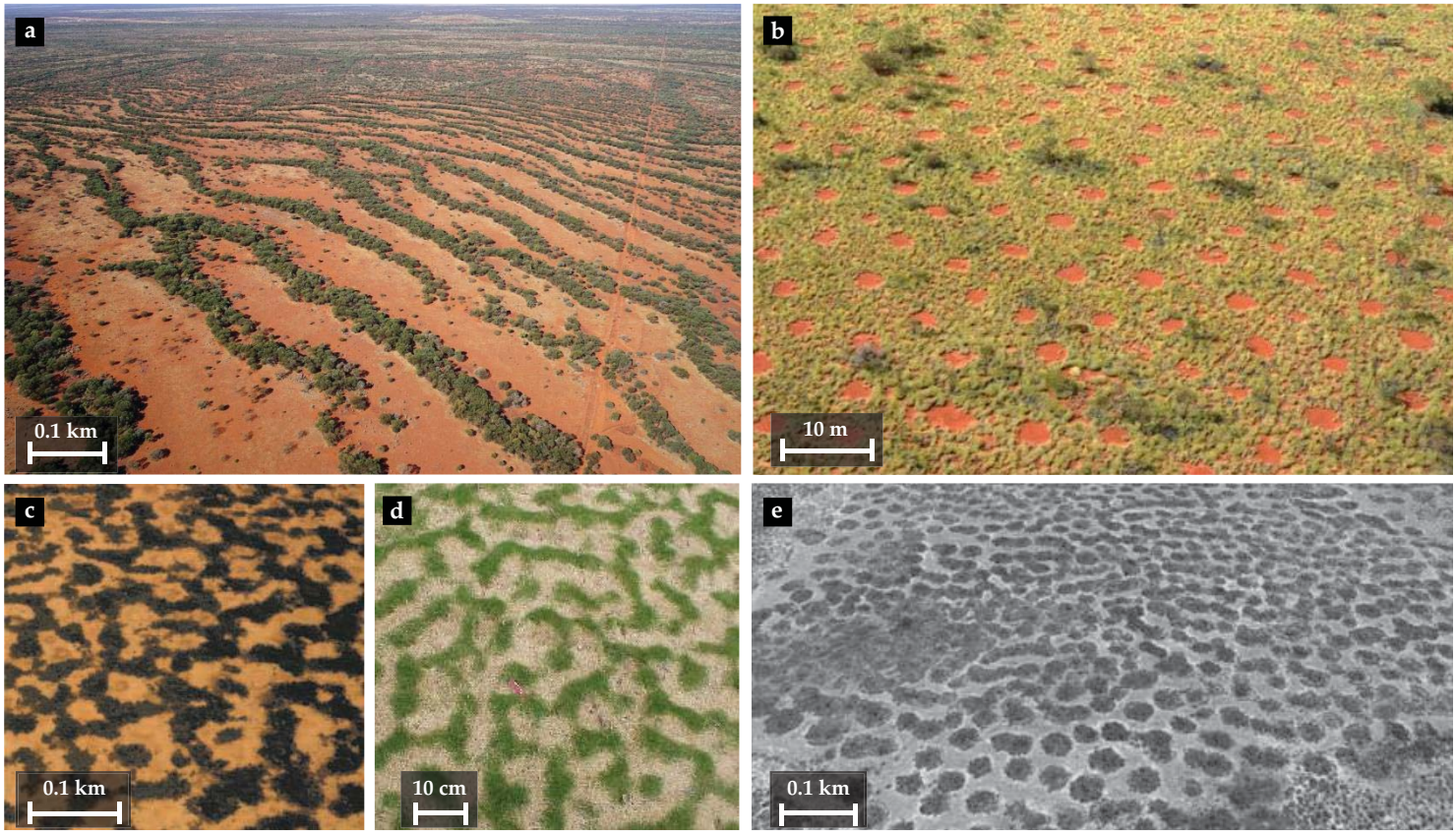

FIGURE 1. DRYLAND VEGETATION can form a range of patterns. **(a)** Banded woody vegetation on a sloped terrain in Australia (photo courtesy of Stephan Getzin). **(b)** A gap pattern of herbaceous vegetation in Australia (from ref. 11). **(c)** A labyrinthine pattern of woody vegetation in Niger (from ref. 4). **(d)** A labyrinthine grass pattern in Israel (from ref. 10). **(e)** A spot pattern of woody vegetation in Zambia (from ref. 18).

In a time when aerial photographs, let alone satellite images, of remote regions were hardly available, Turing could not have imagined the possible realizations of his predictions for dryland vegetation. Those who have traveled through arid and semiarid regions may have noticed the patchy character of the landscape, which is made up of vegetation patches surrounded by bare-soil areas or vice versa. Usually the patchiness appears irregular, which has traditionally been attributed to variable microtopography and soil heterogeneities. It came as a big surprise when aerial photographs of dryland regions, first in East Africa[5] (even before Turing's paper) and later in many regions across the world, revealed strikingly regular vegetation patterns with various morphologies that were not recognizable from the ground.

The first morphology to receive extensive scientific attention was parallel vegetation bands on gently sloped terrains,[6–8] a recent example of which was observed in northwestern Australia (see figure 1a). In flat terrains, additional morphologies have been reported, including nearly hexagonal vegetation gap patterns (figure 1b), labyrinthine stripe patterns (figures 1c and 1d), and nearly hexagonal spot patterns (figure 1e). As figures 1c and 1d show, the same type of pattern can appear with different plant species and on characteristic length scales that vary by orders of magnitude.

Vegetation patterns are not limited to drylands.[4] Recently they have also been observed in underwater seagrass maps obtained using hydroacoustic techniques.[9] The growing recognition of vegetation pattern formation as a fundamental phenomenon observed worldwide with different plant species has led to the emergence of a vigorous new research field at the interface between spatial ecology, nonlinear physics, and applied mathematics,[10] where Turing's ideas are essential.

Positive water–biomass feedback

The spontaneous appearance of large-scale spatial order is often a result of a local positive feedback loop that amplifies small perturbations throughout the whole system and thereby induces an instability of the original state. But what positive feedback loop could drive the formation of the observed periodic vegetation patterns? Assuming that pattern formation in water-limited ecosystems can be explained solely in terms of vegetation growth and water availability, researchers have proposed a feedback loop, illustrated in figure 2, in which water transport toward locations of growing vegetation accelerates vegetation growth that, in turn, enhances the water transport.[4,10,11]

An instability driving uniform vegetation to become patterned can then be understood as follows: Consider a landscape of almost uniform vegetation and an area with slightly denser vegetation than its surroundings. That area draws slightly more water than its surroundings and becomes even denser. The amplified deviation from the originally uniform vegetation closes the feedback loop and sets the ground for a

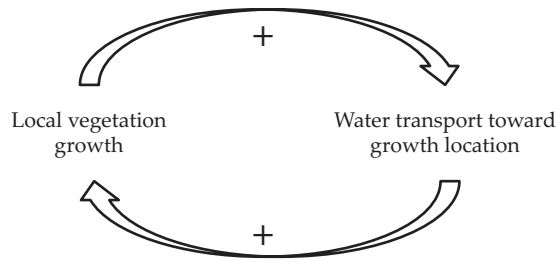

FIGURE 2. A POSITIVE FEEDBACK LOOP drives vegetation pattern formation in water-limited systems. Feedback mechanisms accelerate vegetation growth in denser patches and inhibit growth in adjacent sparser patches, and thereby promote vegetation pattern formation. (Adapted from ref. 10.)

new amplification loop. While the transport of water toward denser vegetation accelerates the growth there, it inhibits the growth in the surrounding areas from which water is being taken. The instability that results generates nonuniform vegetation growth and the formation of a pattern.[4]

The first part of the feedback loop (the lower arrow in figure 2) is fairly obvious in ecosystems where the limiting growth factor is water availability. But why should vegetation growth enhance water transport (the upper arrow)? The answer depends on the particular transport mechanism.

One possible process is overland water flow, shown in figure 3a. Bare-soil areas in drylands are often covered by physical or biogenic crusts that reduce the infiltration rate of surface water into the soil. As a consequence, the infiltration rates in sparsely vegetated areas are lower than those in densely vegetated areas. Further contributing to that infiltration contrast are the plants' roots, which increase the soil porosity and thus the infiltration rate around the plants. The higher rate that develops as the vegetation grows denser in a given location enhances overland water flow toward that location, and that can account for the portion of the feedback loop indicated by the upper arrow in figure 2.

Another mechanism is conduction by laterally extended plant roots (see figure 3b). The biomass of a plant consists of an aboveground part, or shoot, and a belowground part, or root. Those two entities are not independent—larger shoot means larger root; their relationship is expressed in terms of the root-to-shoot ratio. As the shoot grows, the lateral extension of the root zone enhances water transport because it allows for water uptake and conduction from a larger volume.

The root-to-shoot relationship also is essential in enhancing water transport for laterally confined roots (see figure 3c). In that transport mechanism, water diffuses through the soil toward locations of accelerated vegetation growth. Stronger water uptake by deeper roots depletes the water content relative to the surrounding soil and creates soil-water gradients, which induce diffusion.

The three mechanisms are each associated with a positive feedback loop that can induce a pattern-forming instability on its own. In general, the feedback loops can act in concert, and their relative importance changes with environmental conditions. The interplay between them has interesting implications for community structures because of the different water distributions associated with each transport mechanism and the niches those distributions provide for other species.[10,11] The feedback loop associated with overland water flow acts to increase the soil-water content in a vegetation patch, whereas those loops associated with water diffusion and conduction by lateral roots act to decrease that content by their strong water uptake. In landscapes consisting of shrubs and annual plants, dominance of the overland water flow feedback loop can facilitate annuals growing near or under the canopies of shrubs; dominance instead of feedback loops involving strong water uptake can result in the exclusion of annuals from the vicinities of shrubs.[11,12]

Upscaling information from local to global

The biomass–water feedback loops describe local plant-scale processes. But does that small-scale information translate to large-scale collective behaviors? Specifically, can the capabilities of the biomass–water feedback loops induce pattern-forming instabilities in uniform vegetation?

One indispensable tool for addressing such questions is a heuristic mathematical model, built so as to capture the feedback loops associated with overland water flow, water conduction by laterally extended roots, and water transport by diffusion.

Two types of modeling approaches are primarily used to study plant population dynamics: discrete agent-based models, also called individual-based models, and those based on continuum partial differential equations (PDEs). Agent-based models are stochastic computational algorithms that go down to the level of individual plants and often describe each plant in great detail. PDE models, on the other hand, do not address individual plants; rather, they describe deterministic processes at small spatial scales. A plant population is then represented by a continuous biomass areal density.

The PDE approach is more heuristic but has the advantage of lending itself to the powerful methods of pattern-formation theory.[10] But is it a suitable approach to describe small populations of discrete entities, for which demographic noise and extinction are usually a concern? The answer is definitely positive. Unlike animals, plants are immobile organisms that cannot migrate away from environmental stresses. Instead, they generally cope by changing their phenotype. That plasticity is reflected in, among other things, the ability of a single plant to change its viable biomass by orders of magnitude; such flexibility justifies embodying vegetation biomass as a continuous variable. Another consideration that supports the continuum modeling approach is the near irrelevance of extinction events; even in cases of complete plant mortality, long-lived seeds have nonvanishing probabilities of germinating whenever the biotic and abiotic conditions allow and can revive the population.

In 2004 Erez Gilad and colleagues introduced a PDE model that captures all three feedback loops.[12] It contains a biomass variable $b(x,t)$ that quantifies the aboveground areal density of the plant population, and additional biomass variables in the case of a plant community consisting of several populations. There are also two water variables: One describes the soil's water content, $w(x,t)$; the other, the overland water height, $h(x,t)$. Because of the nonlocal nature of water uptake, the model includes integrals over a localized root-kernel function, $g(x,x')$, that captures the lateral root distribution of a plant. Thus the term that describes biomass growth in the biomass equation contains the integral $\int g(x,x')w(x')dx'$, which accounts for plant

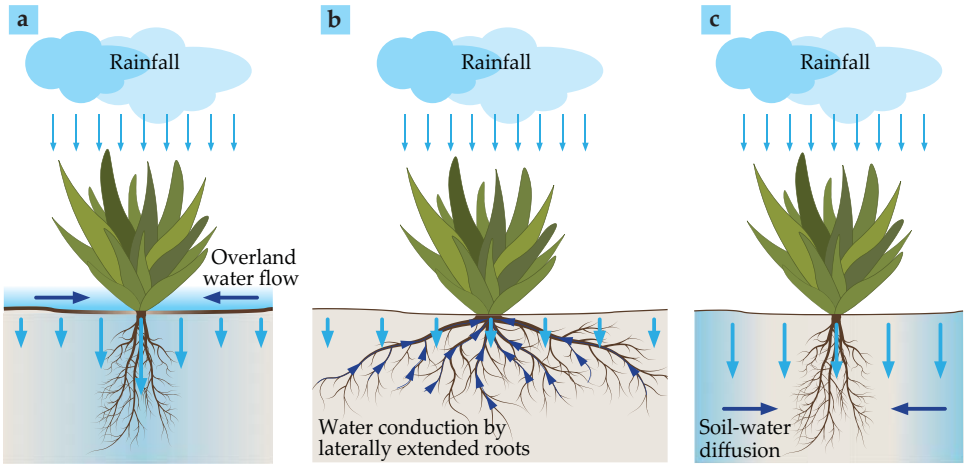

FIGURE 3. THREE FORMS OF WATER TRANSPORT promote flow toward vegetation patches. **(a)** Overland water flow is induced by differences in water infiltration, which is low in bare-soil areas covered by soil crusts, indicated here by a thick ground-surface line, and high in vegetated areas. **(b)** Laterally extended root systems allow plants to increase their water uptake by drawing from a larger volume. **(c)** Water diffuses from water-rich soil in nonvegetated areas with high infiltration rates to water-poor soil in vegetated areas. Dark-blue arrows denote water transport toward growing vegetation. Short light-blue arrows denote low surface-water infiltration rates, and long light-blue arrows denote high infiltration rates. Shaded blue in the soil denotes high water content.

growth at x due to water availability w at all other locations x' in the root zone of x. Likewise, the soil-water equation contains the integral $\int g(x',x)b(x')dx'$, which captures water uptake at x by all plants whose roots extend to that point.

The positive feedback loop associated with laterally extended roots is captured by making the width of the localized root kernel g increase monotonically with the aboveground biomass b, which accounts for the root-to-shoot relation.[12] Water infiltration variability is included in the model by making the infiltration rate of overland water into the soil biomass-dependent; the infiltration rate is higher in more densely vegetated areas.[4]

Applications of the general model to specific ecological contexts often allow simplifications. For example, a model for species with confined root zones can be simplified by using delta-function root kernels; that assumption results in the replacement of the nonlocal integral terms by local algebraic functions. A model for ecosystems with sandy soil characterized by high infiltration rates can be simplified by eliminating the overland-water equation.[10]

PDE models of dryland ecosystems often oversimplify the complex ecological reality and leave aside many factors, such as the effect of transpiration on the atmosphere, soil erosion and deposition, and various plant-physiology processes. They should be viewed as tools that can provide deep insights into given ecological contexts rather than make quantitative forecasts. The models also constitute an indispensable source of well-grounded hypotheses for empirical studies. Such studies are typically long running because of the time scales on which vegetation grows; the hypotheses being tested should therefore be carefully chosen.

Emergence of large-scale periodicity

Analytical and numerical studies of the model discussed above have shown that all three biomass–water feedback loops can induce a nonuniform stationary instability of uniform vegetation when the precipitation rate p drops below a critical value p_T. Such an instability is characterized by the monotonic growth of a spatially periodic mode and the formation of a periodic or nearly periodic stationary pattern.[11] The characteristic wavenumber k_c of the growing mode depends on intrinsic ecosystem properties such as the root-to-shoot ratio and the infiltration contrast.

A convenient way to graphically describe the model solutions and show their existence and stability ranges is to draw a bifurcation diagram such as the one in figure 4a. The horizontal axis represents a control parameter—here the precipitation rate p—and the vertical axis represents a suitable measure of a chosen state variable, such as the biomass spatial average $\langle b \rangle$ or its L^2 norm $\|b\| \propto \int |b|^2 dx$. A common convention in such diagrams is to represent stable solutions with solid lines and unstable solutions with dashed lines.

Figure 4a shows a bifurcation diagram of stationary solutions in one spatial dimension. The simplest solutions, shown in orange, are constant; they represent bare soil ($b = 0$) and uniform vegetation. The bare-soil solution is stable for low precipitation, at which seeds do not germinate, but it becomes unstable at some threshold p_U. Above that threshold a spatially uniform mode begins to grow and drives the system toward a uniform vegetation state. But that state is stable only at sufficiently high precipitation values $p > p_T$. If the precipitation decreases below that threshold, uniform vegetation becomes unstable. Unlike the uniform mode that grows beyond the bare-soil instability, the mode that grows below p_T is spatially periodic (figure 4b). That drives the system toward a stable periodic pattern (the green line in figure 4a).When $p_U < p_T$, as is the case in figure 4a, the destabilization of the bare-soil state above p_U results in a convergence to the periodic-pattern state because the uniform vegetation state is unstable.

In addition to the periodic solution that emerges from the uniform vegetation solution branch at $p = p_T$, the bifurcation diagram shows another periodic solution, indicated by the blue line, that emerges from uniform vegetation at a slightly lower precipitation threshold. Figure 4c shows an example of that periodic solution, which is characterized by a lower wavenumber. That solution extends to the highest precipitation rate, p_H, at which periodic solutions exist. Many additional periodic solutions that are not shown in the figure also appear with decreasing wavenumber as the precipitation decreases further. The last solution is a single hump (figure 4d), indicated by the purple line, which describes a single vegetation spot. That solution extends to the lowest precipitation value p_L at which viable vegetation still exists. Empirical indications of periodic patterns with different wavenumbers have recently been reported.[13]

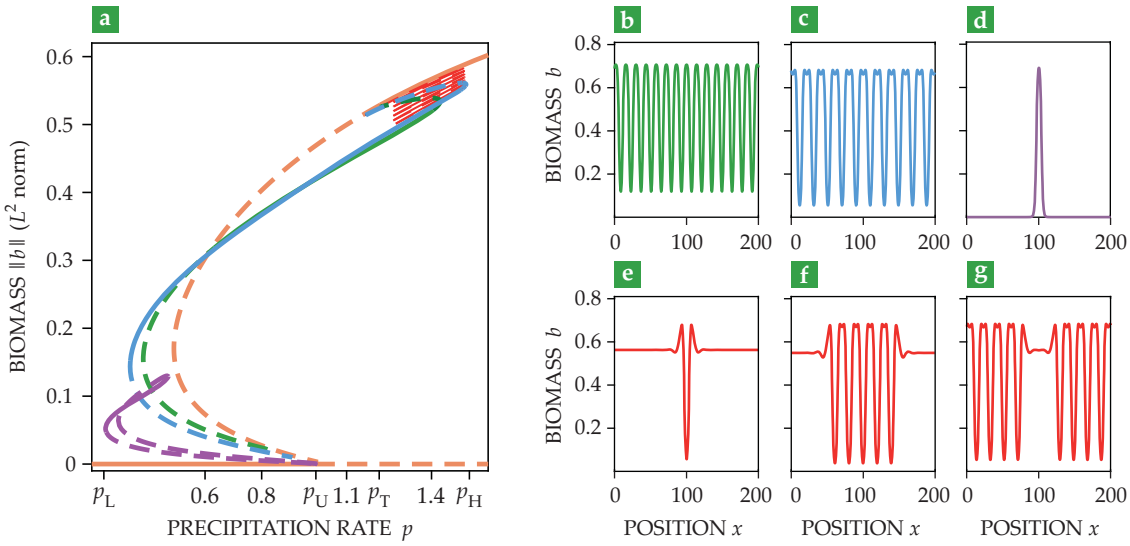

FIGURE 4. PERIODIC AND LOCALIZED PATTERNS emerge from a nonuniform instability of uniform vegetation. **(a)** A bifurcation diagram of one-dimensional solutions of a two-variable model that shows the dependence of the L^2 norm of the biomass b on the precipitation rate p.[11] Solid lines represent stable solutions and dashed lines represent unstable solutions. The orange lines denote two constant solution branches: bare soil with $\|b\| = 0$, which is unstable for $p > p_U$, and uniform vegetation, which is unstable for $p < p_T$. The green line represents the periodic solution that bifurcates from the uniform-vegetation solution at p_T. The blue line represents the periodic solution that extends to the highest precipitation value p_H. The purple line denotes a single-hump solution with zero wavenumber and defines the lowest precipitation value, p_L, at which spatial patterns exist. The branches of the snaking red line represent localized solutions of different sizes. **(b–g)** Spatial dependencies of solutions that correspond through their colors to the various branches in panel a. Numerical values refer to dimensionless quantities. The corresponding dimensional quantities are $P = p \cdot (160\ \text{mm/yr})$, $B = b \cdot (1\ \text{kg/m}^2)$, and $X = x \cdot (1 / 10\sqrt{2}\ \text{m})$. (Courtesy of Yuval R. Zelnik.)

The green and blue periodic-solution branches that emerge from the uniform vegetation solution appear in subcritical bifurcations—that is, a precipitation range exists where both uniform vegetation and periodic patterns are stable states. That range extends from the threshold p_T, at which the uniform vegetation state loses stability, to a threshold beyond which periodic solutions cease to exist (see figure 4a).

Within that range there exist a multiplicity of stable localized patterns of increasing size, beginning with a gap in otherwise uniform vegetation (figure 4e), through gap-pattern domains of increasing sizes (figure 4f), to a periodic gap pattern with a single missing gap (figure 4g). In figure 4a, those localized patterns are denoted by the red curve that snakes back and forth between the uniform and the periodic solution branches; that behavior has been termed homoclinic snaking.[14] The localized patterns act as building blocks for many irregular but stable patterns that are hybrids of uniform vegetation and periodic gap patterns. Empirical indications of such hybrid patterns have been reported in studies of grassland gap patterns in Namibia.[15]

In two-dimensional isotropic systems, nonuniform stationary instabilities generally result in the emergence of periodic hexagonal patterns. Such patterns are formed by the simultaneous growth of three resonant modes with wavevectors of the same magnitude k_c but oriented 120° relative to each other.[10] Indeed, simulations starting from a nearly uniform vegetation state slightly below p_T result in a nearly hexagonal gap pattern, as figure 5 shows. Such dynamical behavior has been used to explain observed hexagonal gap patterns in Australian grasslands, shown in figure 1b, and how they differ from apparently similar hexagonal gap patterns in Namibian grasslands.[16]

Ecosystems with sloped terrains are not isotropic, and the patterns that emerge from simulations are mostly stripes oriented perpendicular to the slope. That finding is consistent with empirical observations,[8] such as the stripes in figure 1a. In fact, in sloped terrains, the instability of uniform vegetation involves the oscillatory growth of a spatially periodic mode,[10] which results in vegetation bands migrating uphill.[17] That migration, which has been empirically confirmed,[8] can be understood as a result of the better growth conditions for plants at the top of a vegetation band, where runoff accumulates, than at the bottom part, where runoff is lost.

A basic principle for vegetation patterning

The emergence of periodic patterns from uniform vegetation as the rate of precipitation decreases can be viewed as a population-level mechanism—one that involves many individual plants—to cope with the water stress caused by reduced rainfall. Partial plant mortality and the concomitant formation of bare-soil gaps create an additional water source for the surrounding vegetation through the various forms of water transport illustrated in figure 3. The water contributed by bare-soil areas to surrounding vegetation compensates for the reduction in direct rainfall and allows for the survival of the remaining vegetation patches. The utility of that principle shows up in the system's response to further reductions in rainfall: Less rain should result in larger bare-soil areas capable of contributing more water to adjacent vegetation patches. That area increase is indeed observed in simulations, and it can be realized in different ways.

The simplest mechanism by which bare-soil areas can increase is by a contraction of vegetation patches. In one-dimensional patterns, such as banded vegetation on sloped terrains, that

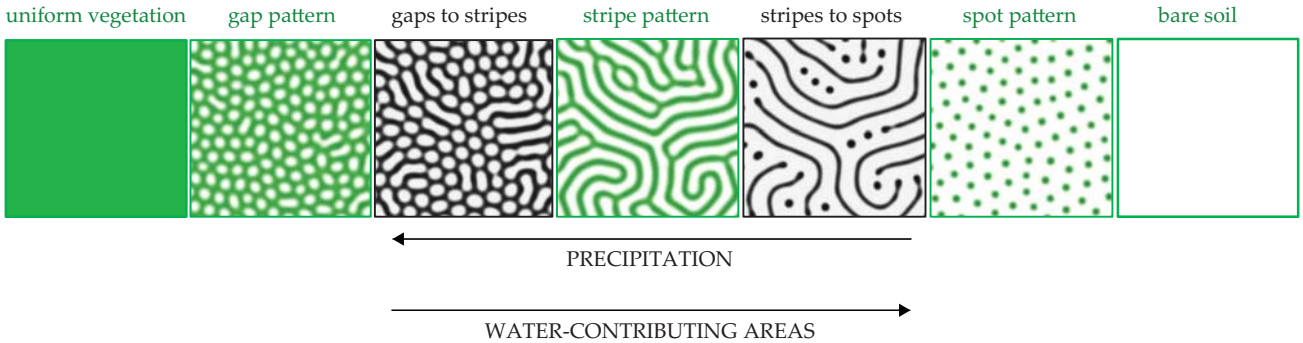

FIGURE 5. THE FIVE BASIC VEGETATION PATTERNS along the rainfall gradient (green panels) and snapshots of two morphological transitions (black-and-white panels) as obtained by model simulations with slowly decreasing rates of precipitation. As precipitation decreases from left to right, bare-soil areas, which contribute water to adjacent vegetation areas, should increase in size for the vegetation to remain viable. That increase results in two morphological transitions: Gaps become stripes through the merging of bare-soil gaps, and as vegetation disintegrates further, those stripes turn into spots.

contraction amounts to vegetation bands narrowing while their number stays constant, which keeps the pattern's wavenumber unchanged. That response mechanism occurs along the branch of any periodic solution, such as the green and blue lines in figure 4a. Those solution branches extend to precipitation values lower than that of the uniform-vegetation solution (upper orange line), which manifests the positive effect of vegetation patterning and band thinning on the vegetation's capacity to survive water stress. Another way in which bare-soil area can increase in response to decreasing precipitation is through a reduction in the number of vegetation patches. That response is reflected in transitions to periodic solutions with lower wavenumbers as p decreases.

Two-dimensional patterns have yet another mechanism for increasing bare-soil area in response to decreasing rainfall: the morphological transitions illustrated by the black-and-white panels in figure 5. The first transition involves the merging of adjacent bare-soil gaps in a hexagonal pattern to form bare-soil stripes. The resulting pattern persists to lower precipitation values until a second morphological transition takes place in which stripes break into spots. Those two transitions, together with the instability of uniform vegetation to hexagonal gap patterns and the collapse of spots to bare soil, form a sequence of five basic vegetation states along the rainfall gradient, shown by the green panels in figure 5.

From patterns to function

The discussion so far has focused on understanding mechanisms of vegetation pattern formation and accounting for the variety of patterns observed in drylands. But beyond the obvious curiosity raised by those fascinating phenomena, there are important open questions related to functional aspects of vegetation patterning that call for further study. The functioning of dryland ecosystems is currently threatened by two main factors. The first is global climate change and the likely more frequent extremes, such as severe droughts, that accompany it; the second is human intervention, which often involves extracting resources, such as livestock feeding, and imposes additional stresses on already vulnerable ecosystems.

Climate extremes can cause abrupt and irreversible transitions in vegetation that lead to alternative dysfunctional stable states, such as bare soil. How do the many stable vegetation pattern states affect such transitions? Can they mitigate the effects of extreme droughts by providing alternative vegetation response pathways that culminate in functional patterned states rather than collapse to bare soil?

Human intervention also often results in detrimental outcomes. But whereas researchers need to understand the many stable ecosystem states to address the effects of climate extremes, they have to study unstable ecosystem states to deal with human intervention. Directions in which an ecosystem departs from its unstable states can act as road signs for judicious human interventions. Following those signs may circumvent detrimental outcomes by directing ecosystems toward functional states. However, identifying the relevant unstable states for particular human interventions remains a challenge.

Understanding the transient dynamics of dryland ecosystems caused by climate extremes and human intervention calls for interdisciplinary collaborations between physicists, applied mathematicians, and ecologists. By working together, they can assimilate the concepts and methodologies of pattern formation into ecological theories and facilitate research progress.

REFERENCES

1. A. Turing, *Philos. Trans. R. Soc. Lond. B* **237**, 37 (1952).
2. V. Castets et al., *Phys. Rev. Lett.* **64**, 2953 (1990).
3. Q. Ouyang, H. Swinney, *Nature* **352**, 610 (1991).
4. M. Rietkerk, J. van de Koppel, *Trends Ecol. Evol.* **23**, 169 (2008).
5. W. Macfadyen, *Geogr. J.* **116**, 199 (1950).
6. R. Lefever, O. Lejeune, *Bull. Math. Biol.* **59**, 263 (1997).
7. C. Klausmeier, *Science* **284**, 1826 (1999).
8. V. Deblauwe et al., *Ecol. Monogr.* **82**, 3 (2012).
9. D. Ruiz-Reynés et al., *Sci. Adv.* **3**, e1603262 (2017).
10. E. Meron, *Nonlinear Physics of Ecosystems*, CRC Press/Taylor & Francis (2015).
11. E. Meron, *Annu. Rev. Condens. Matter Phys.* **9**, 79 (2018).
12. E. Gilad et al., *Phys. Rev. Lett.* **93**, 098105 (2004).
13. R. Bastiaansen et al., *Proc. Natl. Acad. Sci. USA* **115**, 11256 (2018).
14. E. Knobloch, *Annu. Rev. Condens. Matter Phys.* **6**, 325 (2015).
15. Y. R. Zelnik, E. Meron, G. Bel, *Proc. Natl. Acad. Sci. USA* **112**, 12327 (2015).
16. S. Getzin et al., *Proc. Natl. Acad. Sci. USA* **113**, 3551 (2016).
17. J. A. Sherratt, *J. Math. Biol.* **51**, 183 (2005).
18. F. Borgogno et al., *Rev. Geophys.* **47**, RG1005 (2009).

PT